Chapter 5

Application of sol-gel derived $BaTiO_3$ thin film as gate dielectric of SnO_2 thin film transistor

5.1 Introduction-

Metal oxide thin-film transistors (TFTs) research have received enormous attention in the last two decades because of the possibility of their application in various technological area including display technology, transparent and flexible electronics, large-area sensor, etc.[192-194] Gate dielectrics thin film is a major component of an oxide TFT which demands increasing gate capacitance, excellent interface with metal oxide semiconductor, and the crystalline orientation of semiconductor layers on dielectrics to provide higher performance and faster carrier transport qualities.[195, 196] High capacitance thin film for gate dielectric can be obtained either from thinner film or from high dielectric constant (high-k) materials. So far, numerous inorganic high-k metal oxide materials, including magnesium oxide, titanium dioxide, zirconium oxide, hafnium oxide [197-200], etc. have been employed in integrated circuit manufacturing and experimental study as high-permittivity materials. Besides these, titania-based perovskite materials are also getting interested due to their high dielectric constant as well as their ferroelectric behavior.[201-203] Among them, barium titanate ($BaTiO_3$) is one of the most studied materials as lead-free perovskite that has ferroelectric behavior below Curie temperatures (130˚C) and has a 3.2 eV broad bandgap, indicating good insulating properties.[204, 205] It has also been used as a gate insulator for numerous organic thin-film transistors and oxide heterojunction transistors.[180, 181, 206, 207] In most of these works, $BaTiO_3$ has been deposited in various physical vapor deposition techniques.[203] Therefore, a method for a solution-processed barium titanate thin film deposition is urgently required for the low cost and large-area fabrication of this material.

In my thesis work, I have synthesized $BaTiO_3$ thin film by a solution-processed technique that is compatible with large-area fabrication. The surface morphology study of this film shows the smooth nature of the film. The electrical measurement of this thin film shows its insulating nature of this film. A solution-processed tin oxide (SnO_2) thin-film transistor (TFT) has been fabricated by using this BaTiO3 thin film. This SnO_2 TFT can run within 5.0 V external voltage with reasonably good carrier mobility. Details of this study have been discussed in the following section.

5.2 Device fabrication-

The SnO_2 TFTs with $BaTiO_3$ gate dielectric were made on a p^{++}-Si substrate as discussed in chapter-2. The substrate was first to wet cleaned with an ultrasonic bath before being treated with oxygen plasma. After that, the $BaTiO_3$ precursor solution was spin-coated on p^{++}-Si substrates for 40 seconds at 4000 rpm, then annealed for 30 minutes at 350˚C. This coating process was repeated one mere time followed by final annealing for 1 hour at 850˚C to get the polycrystalline coating of $BaTiO_3$ thin film. A metal-insulator-metal (MIM) structure capacitor was made by evaporating Al on the surface of $BaTiO_3$ thin films to investigate its electrical and dielectric characteristics. For TFTs fabrication, a precursor solution of SnO_2 was spin-coated onto the p^{++}-Si/$BaTiO_3$ substrate followed by an annealing step at 500˚C for 30 minutes. Thermally deposited aluminum was used as source/drain electrode and was coated on top of SnO_2 layer through a shadow mask process with a wide-to-length (W/L) ratio of 118.

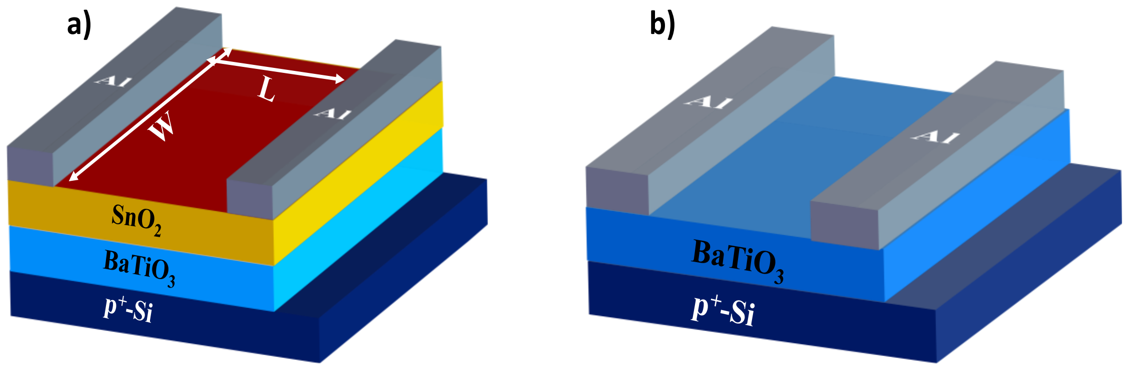

Figure 5.1: Device Layouts of a) Schematic of solution-processed metal-oxide TFT b) MIM structure.

5.3 Result and Discussion

5.3.1 Thermal analysis-

The thermal behavior of sol-gel-made $BaTiO_3$ powder was investigated using thermos-gravimetric analysis (TGA) in a nitrogen atmosphere at a heating rate of 20˚C /min from ambient temperature to 1000˚C as shown in **figure 5.2**. The first weight reduction (12.5 percent) from 123˚C to 395˚C can be attributable to the decomposition of precursor salts, loss of physical adsorption water molecules, and disintegration of organics components such as 2-methoxy ethanol. The second one was observed between 817˚C - 987˚C which is the breakdown of remaining organics resulting in the loss of 4% of the mass. Weight loss between 817˚C and 987˚C is continuously increasing which implies that $BaTiO_3$ has a wide crystallization window.

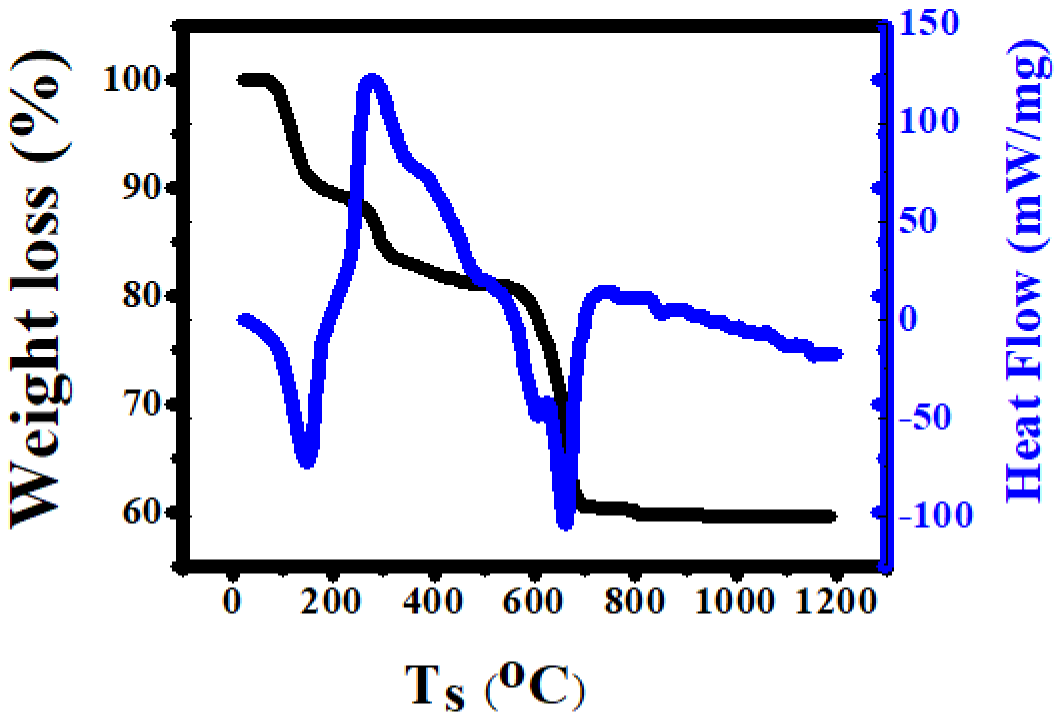

Figure 5.2: TGA and DTA of $BaTiO_3$ thin film annealed at 750˚C.

5.3.2 Structural properties of $BaTiO_3$ powder-

XRD analysis was performed on the sol-gel prepared powder sample heated at 850˚C for three hours to confirm $BaTiO_3$ crystal formation, and the results are given in **figure 5. 3** To get a powder sample with complete crystallization, a longer annealing period is necessary. The data indicates a definite $BaTiO_3$ crystal growth at this temperature. The cubic crystal phase of $BaTiO_3$ is confirmed by the diffraction peaks at 2θ angles of 22.1°, 31.4°, 38.7°, 45.0°,50.7°, and 56.6°, which correspond to planes of reflections of (100), (110), (111), (200), (210), and (211), respectively (JCPDS, No. 892475)

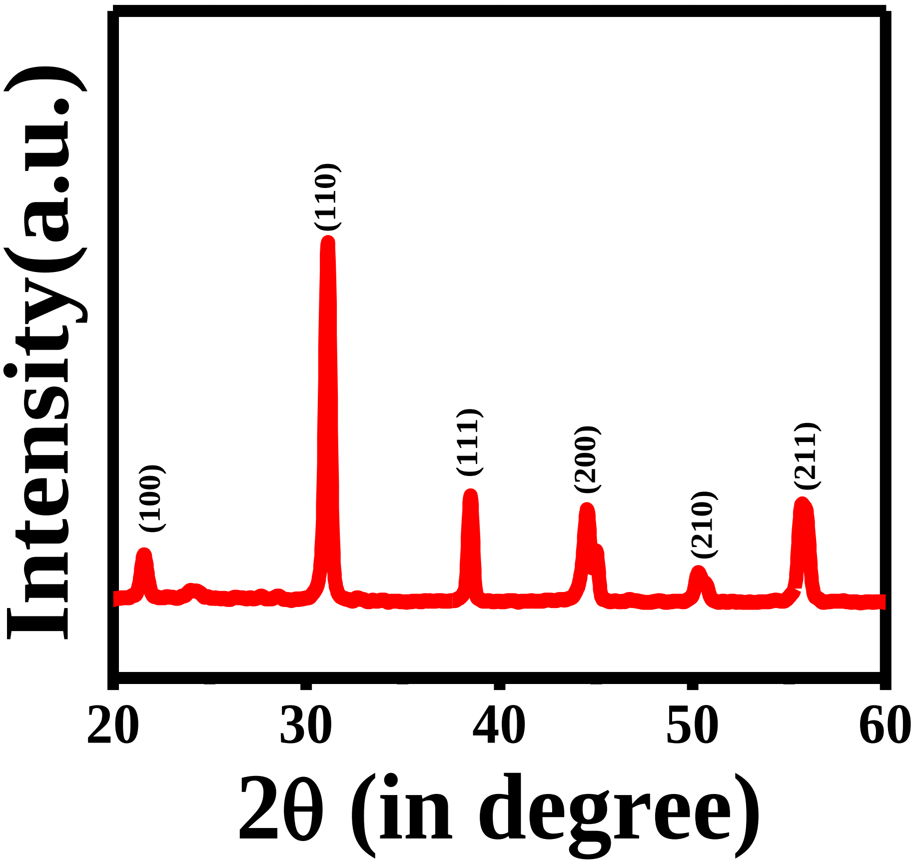

Figure 5.3: XRD pattern of $BaTiO_3$ Powder

5.3.3 Optical Properties of Dielectric $BaTiO_3$ Thin Films-

For the optical transparency study, a thin film of $BaTiO_3$ was deposited on a quartz substrate under the same circumstances as TFT dielectric thin film was coated. **Figure 5.4** shows the average transmittance value is above 90% through the visible region. The optical band gap of $BaTiO_3$ is 3 eV which is extracted from optical data and has been shown in **figure 5.4 b**, which is quite comparable with a previously reported value of 3.2 eV by other groups.[7]

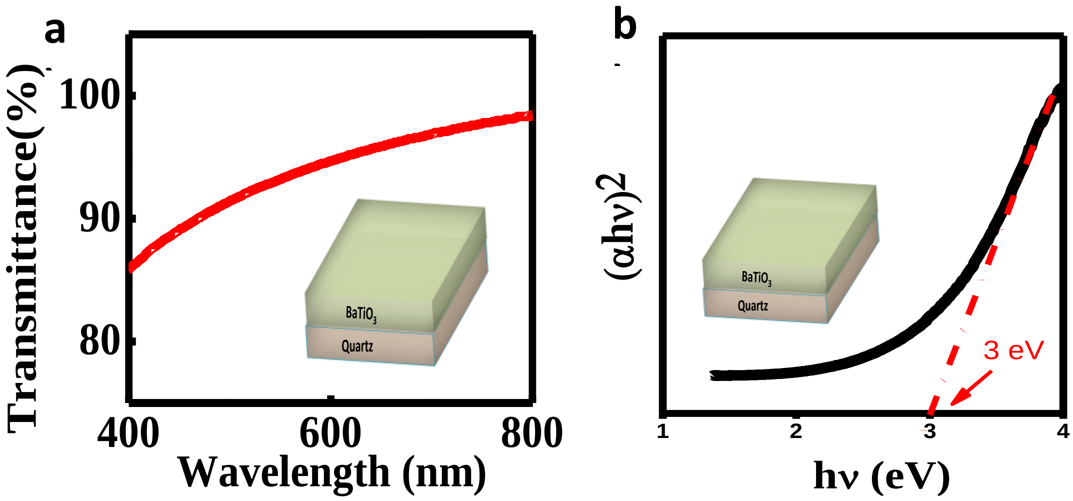

Figure 5.4: a) Optical transmittance spectra, b) optical band gap of $BaTiO_3$ thin film annealed at 750˚C.

5.3.4 Surface morphology-

The dielectric/semiconductor contact is critical for thin-film transistor performance. Therefore, it is important to characterize the surface morphology of dielectric thin films. Because it is well known that rough interfaces (dielectric/semiconductor) operate as a hurdle and obstruct charge carrier transit in semiconductor channels. Atomic force microscopy (AFM) was used to analyze the surface morphology of p^{++}-Si/$BaTiO_3$ and p^{++}-Si/$BaTiO_3$/SnO_2 thin films. The dielectric roughness of p^{++}-Si/$BaTiO_3$ and p^{++}-Si/$BaTiO_3$/SnO_2 is 3.05 nm and 2.58 nm, respectively, which is acceptable for thin-film transistors.

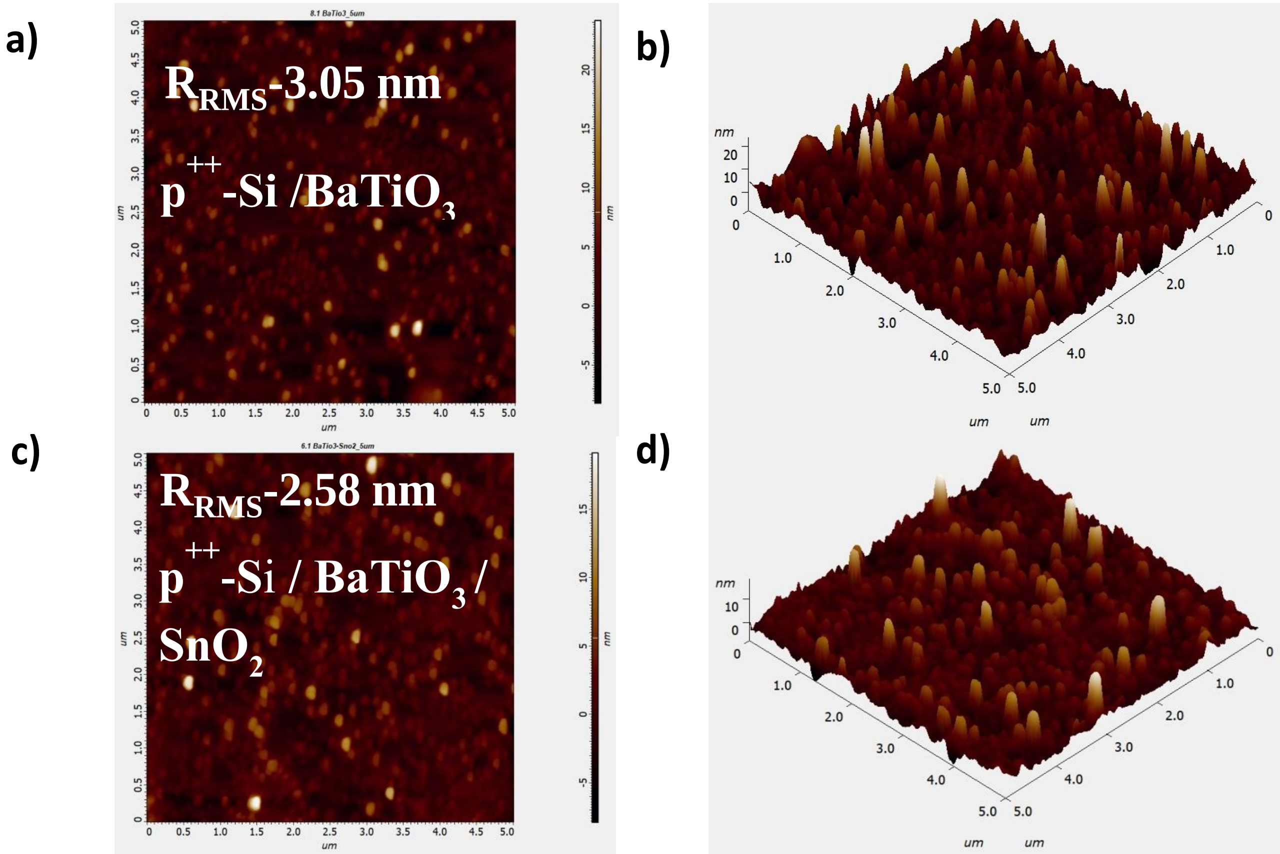

Figure 5.5: 2-D and 3-D Surface morphologies of the solution processed $BaTiO_3$ dielectric thin films for (a), (b), p^{++}–Si/ $BaTiO_3$, (c),(d), p^{++}–Si/ $BaTiO_3$/SnO_2.

5.4 Device characterization

To realize the dielectric properties and the electrical conductivity of the as-deposited $BaTiO_3$ films, frequency-dependent capacitance (C–f) and current-voltage (I–V) measurements were performed in a metal-insulator-metal (MIM) device architecture. The capacitance of a p^{++}-Si/$BaTiO_3$/Al device with a 50 nm thickness $BaTiO_3$ layer is 330 nF cm^{-2} as shown in **figure 5.6 b** The areal capacitance of $BaTiO_3$ thin film remains almost constant up to the frequency of 10 kHz and rapidly falls above 100 kHz. Leakage current densities of 4 x 10^{-4} A/cm^2 were observed in the $BaTiO_3$ dielectric thin film at 5V as depicted in **figure 5.6 a**. The results suggest that $BaTiO_3$ might be used as an insulator of a TFT.

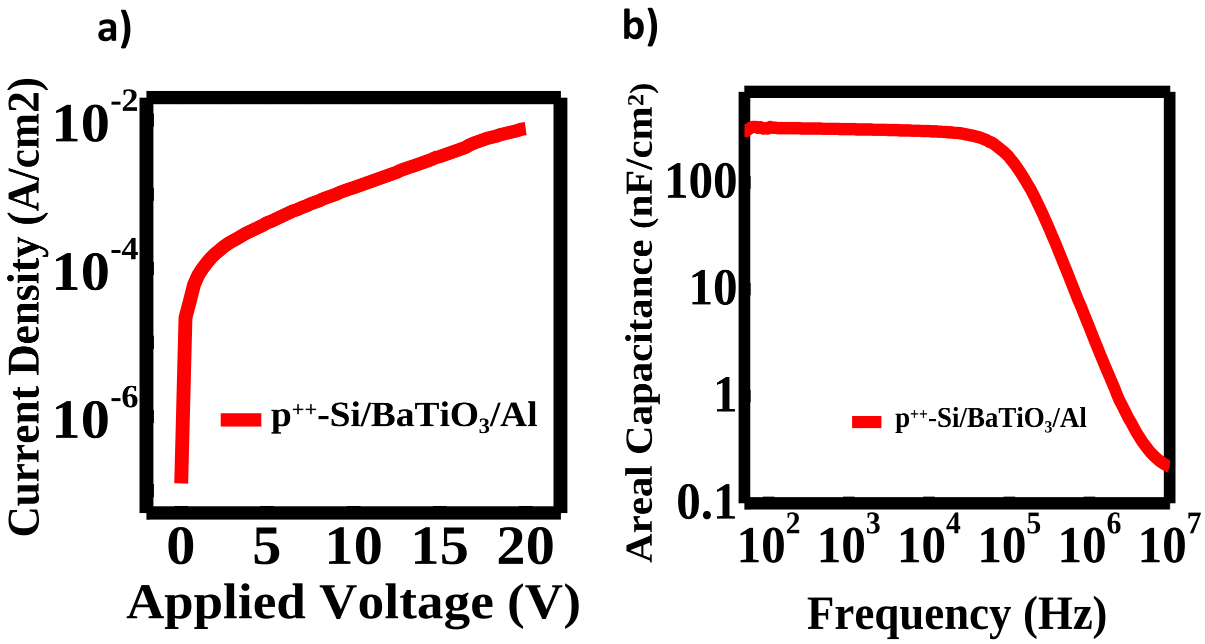

Figure 5.6: Variation of (a) leakage current density v/s applied voltage and (b) capacitance v/s frequency of $BaTiO_3$ gate dielectric with MIM device architecture

Figure 5.7 illustrates the I_D - V_D, and I_D - V_G characteristics of SnO_2 transistors with $BaTiO_3$ gate dielectric, annealed at 850˚C temperature. All of the tests were carried out in an ambient environment. During the output characteristic study, the gate voltage (V_G) was pushed between 0 and 5 V with a 1V step for this TFT device, while the applied drain voltage (V_D) was varies from 0 and 4 V. The linear and saturation zones of the output characteristics are clearly seen in the diagram. The I_D–V_G measurements (transfer characteristics) of the same SnO_2 TFT with a drain voltage (V_D) of 4 V are shown in **figure 5.7 b**. The gate-source voltage (V_G) was changed from -2 V to 5 V. The following equation is used to compute the mobility of this TFT at saturation.

$$I_D = \mu C \frac{W}{2L} (V_G - V_T)^2 \quad ....(1)$$

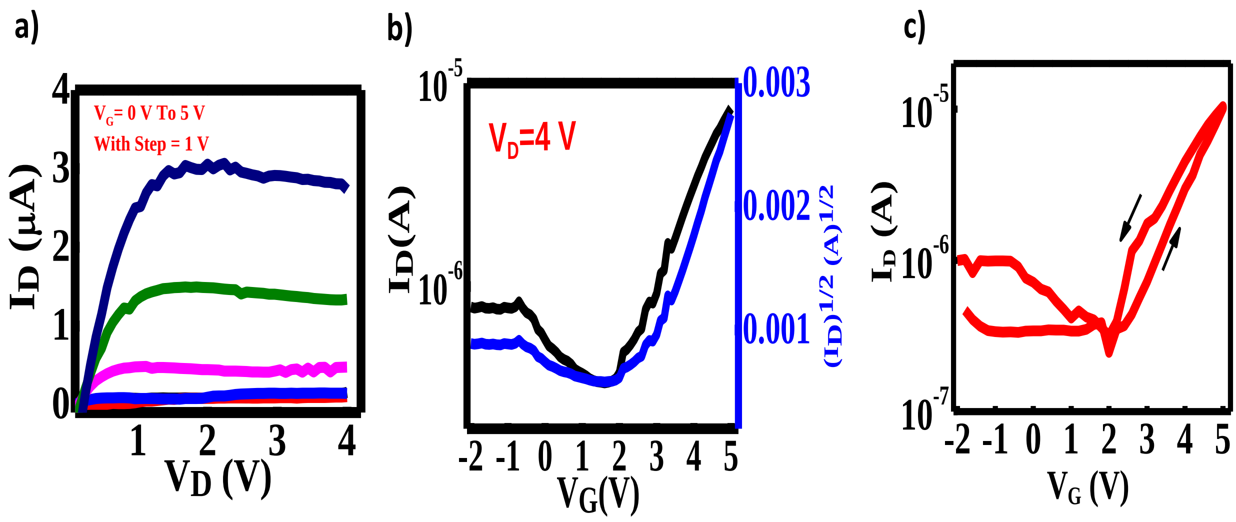

Figure 5.7: (a), (b) Output and transfer characteristics to extract slope for charge carrier mobility calculation for Al/SnO_2/$BaTiO_3$/p^{++}-Si device structure and(c) transfer characteristics with hysteresis.

We used the lower frequency (50 Hz) capacitance for our mobility computation to prevent overestimating mobility. With a capacitance of 330 nF.cm^{-2} at 50 Hz, the obtained on/off ratio of this TFT (from **figure 5.7 b**) is equal to 25 with effective electron mobility of 0.028 cm^2 V^{-1} s^{-1}. The subthreshold swing (S) of this device is 2.2 V/decade.

Interface states determine the quality of surface states as well as the dielectric/semiconductor interface. The interface-states-densities (N_{SS}^{Max}) were computed using the following equation by using the SS value of output characteristics.

$$N_{SS}^{Max} = \left[\frac{SS \times \log e}{\frac{kT}{q}} - 1\right]\frac{C}{q} \quad \text{....................(2)}$$

The Boltzmann constant and electrical charge are represented by k and q, respectively. The values of N_{SS}^{Max} determined was 9 x 10^{13} cm^{-2} which is reasonably low for a solution-processed metal oxide TFT.